Proceedings of the
Annual Stability Conference
Structural Stability Research Council
Atlanta, Georgia, April 21-24, 2026

Influence of elastic buckling characteristics on inelastic shear capacity of steel plate girders

Muhie D. Ahdab[1], Maria E.M. Garlock[2], Spencer E. Quiel[3]

Abstract

Steel I-shaped plate girders commonly rely on slender, stiffened web panels to resist shear, yet the role of initial geometric imperfections in governing their elastic buckling and nonlinear inelastic shear response remains poorly understood. This paper investigates the influence of initial imperfections and web slenderness on the elastic buckling and nonlinear shear behavior of steel plate girder webs. The study is based on a dataset of five web panels from three commercially fabricated girders with field-measured imperfections. Experimentally validated finite element models are used to analyze elastic shear buckling loads, inelastic shear capacities, and associated deformation patterns. Elastic buckling analyses compare the response of models with idealized flat web plates as the initial condition to those with field-measured out-of-flatness imperfections. The results show that elastic buckling loads predicted for imperfect webs are 5 to 7 times larger than those for perfectly flat webs. This indicates that a distinct elastic shear buckling bifurcation is unlikely to occur in real plate girder behavior. Also, the application of different field-measured initial conditions on the same web panel results in similar eigenmode characteristics and negligible differences in V_{cr}. The nonlinear shear response of webs with field-measured initial imperfections can be accurately captured by instead using eigenmode-based initial imperfections. A study on the effects of web slenderness ratio indicates that only at high slenderness do the trends change in terms of the shape of the deformed web at the shear capacity load. Future work will expand the geometric database and provide insights for developing design recommendations that more accurately account for the role of imperfections in the shear response of steel plate girders.

1. Introduction

Steel plate girders are widely used in long-span bridge and building applications because their flexural stiffness and capacity can be efficiently designed by increasing the web depth while reducing the web thickness to minimize self-weight and material use. As a result, the shear resistance will often be a governing limit state for plate girder design. To improve shear performance, transverse stiffeners are welded to the web at regular intervals, thus subdividing the web plate into discrete rectangular *panels* bounded by the flanges and stiffeners (see Fig. 1).

[1] Graduate Research Assistant, Princeton University, <ma1081@princeton.edu>
[2] Daniel Tsui Professor in Engineering, Princeton University, <mgarlock@princeton.edu>
[3] Associate Chair and Associate Professor of Structural Engineering, Lehigh University, <seq213@lehigh.edu>

Web shear behavior in steel plate girders has been studied extensively for over a century (Hingnekar and Vyavahare 2020). Experimental investigations have consistently demonstrated that the shear response of plate girders does not demonstrate classical buckling bifurcation (Kim 2014; Numanović and Knobloch 2025a; Masungi et al. 2025; Basler 1961; Rockey and Skaloud 1968; Hansen 2018; Bergfelt and Hovik 1968; Evans et al. 1978; Narayanan and Rockey 1981; Sakai 1966; Kamtekar 1972; Scandella et al. 2020; Lee and Yoo 1999; Pedro et al. 2025; Nascimento et al. 2025; Freitas et al. 2024). Instead, initial out-of-flatness imperfections develop second-order bending as shear load increases, gradually evolving into a buckled shape that closely resembles an elastic eigenmode (illustrated as W1, W2, or W3 in Fig. 1). The number of half-waves is primarily influenced by the panel aspect ratio, a/h (where a is the stiffener spacing and h is the web depth), as well as by the rotational restraint provided along the panel edges by the boundary elements (denoted as a "frame" in Fig. 1). Deformation patterns with an odd number of half-waves are classified as *symmetric*, while those with an even number are *antisymmetric* (Timoshenko and Gere 2009; Stein and Neff 1947; Chilver 1967; Budiansky 1948; Gerard and Becker 1957; Cook and Rockey 1962a, 1962b; Budiansky et al. 1948; Ahdab et al. 2025).

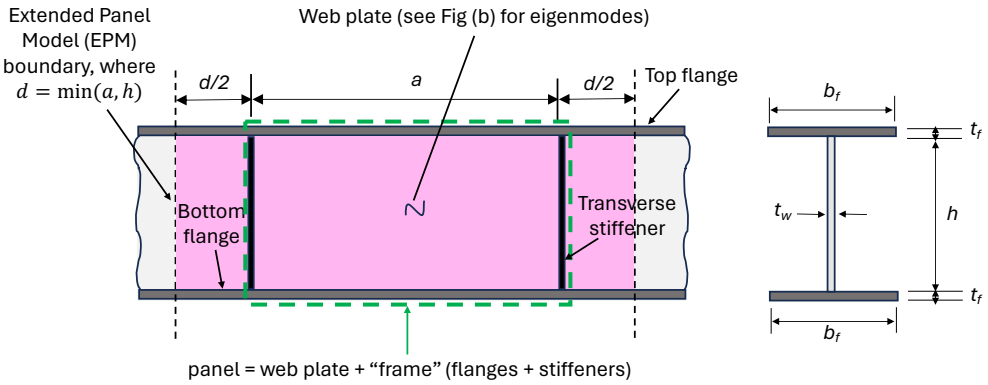

(a) Definition of panel components, geometric variables and EPM modeling approach

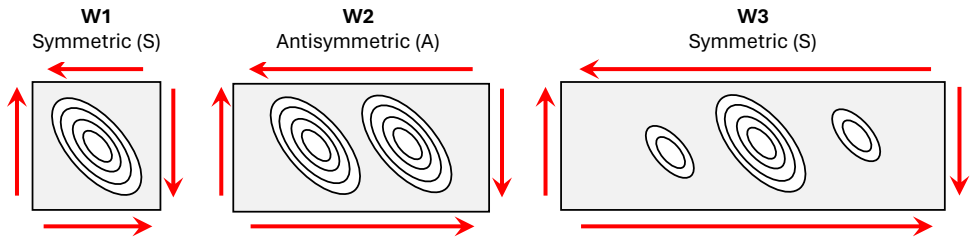

(b) Potential eigenmodes in web plate showing symmetric (W1,W3) and antisymmetric (W2) half-waves

Figure 1: Schematic of a web panel in a plate girder: (a) definitions and (b) eigenmodes.

The elastic shear buckling eigenvalue has long been recognized as an important parameter in the design of stiffened web plates; however, the role of the associated eigenmode shape in determining the inelastic shear capacity has received far less attention. Ahdab et al. (2025) used experimental and numerical evidence to show that the "*eigensystem*", defined by both the eigenvalue and eigenmode shape, used to represent initial imperfections can influence the predicted shear capacity and the inelastic shear response of slender stiffened web plates. Using a large dataset of experimentally validated FE models, that study demonstrated that realistic web panels behave similarly to plates with rotationally clamped (fixed) long edges. Also, the inelastic shear capacity

is influenced more by the final deformed shape (that is, the number of half-waves) that develops as shear load increases than by whether the initial out-of-flatness imperfection corresponds to the first or second eigenmode, a higher order eigenmode, or even a realistically non-uniform field-measured pattern. As a result, that research found that the minimum shear capacity can be associated with either the first or second eigenmode as the initial imperfection, depending on which one produces the governing deformation pattern at inelastic shear capacity.

Building on those findings, the objective of the present paper is to extend the Ahdab et al. (2025) investigation by examining the influence of theoretical elastic buckling characteristics on the realistic nonlinear response of steel plate girders using *field-measured* initial imperfections. Both the elastic shear buckling load, V_{cr}, and the inelastic shear capacity, V_w, of steel plate girder web panels are examined using experimentally validated finite element models. The field-measured imperfections are based on data collected from a steel fabrication shop and reported in prior studies (Masungi et al. 2024a and 2024b; Masungi et al. 2025). Linear eigenvalue analyses are used to examine elastic buckling loads and mode shapes, while nonlinear analyses are performed to characterize the nonlinear shear response and inelastic shear capacity. The influence of web slenderness on both elastic and nonlinear behavior is also examined. Collectively, the results provide new insight into the role of the stiffened web's eigensystem and field-measured out-of-flatness imperfections in shear response. These results show why plate girders do not exhibit classical shear buckling bifurcation behavior, with implications for improved modeling and future design formulations.

2. Background

2.1. Elastic Buckling of Perfectly Flat Web Plates

Theoretical elastic shear buckling behavior of a perfectly flat plate girder web is commonly characterized by the elastic shear buckling load (V_{cr}) (Timoshenko and Gere 2009):

$$V_{cr} = \frac{k_v \bullet \mathrm{E} \bullet \pi^2 \bullet A_w}{12 \bullet (1-\mu^2) \bullet (\frac{h}{t_w})^2} \tag{1}$$

In these expressions, E is the modulus of elasticity, μ is Poisson's ratio, h and t_w are the web depth and thickness, respectively, $A_w = h \cdot t_w$ is the web area, and h/t_w is the web slenderness. The elastic shear buckling load V_{cr} corresponds to the eigenvalue of the shear-loaded system and therefore depends on the boundary conditions through the shear buckling coefficient (k_v).

The first eigenmode (E1) produces the lower-bound solution for k_v and V_{cr} and is thus the basis for design approaches. The second eigenmode (E2) thereby produces a larger solution for k_v and V_{cr}. Fig. 2 illustrates the theoretical solutions for k_v, which are a function of a/h and boundary conditions on the frame (i.e. flanges and stiffeners). Buckling modes are commonly classified as symmetric (characterized by an odd number of half-waves, such as W1 and W3), or antisymmetric (characterized by an even number of half-waves, such as W2) as shown in Fig. 1. As a/h varies, the lower-bound mode E1 can transition between symmetric and antisymmetric configurations, thus producing transition points where the shape of the first eigenmode changes (see Fig. 2).

Classical analytical approaches developed in the mid-twentieth century (such as the Rayleigh–

Ritz, Lagrange multiplier, and matrix iteration methods) have been used to compute theoretical values of k_v for discrete values of a/h and specific boundary conditions of a perfectly flat web plate (Timoshenko and Gere 2009; Stein and Neff 1947; Chilver 1967; Budiansky 1948; Gerard and Becker 1957; Cook and Rockey 1962a, 1962b; Budiansky et al. 1948). In a recent study, Ahdab et al. (2025) demonstrated that these theoretical results can be reproduced using finite element eigenvalue analyses of a web plate subjected to pure shear with idealized boundary conditions. Four boundary conditions were considered for the web plate's framing, and the results are simplified in Fig. 2: (i) all edges simply supported, (ii) all edges fully fixed, (iii) fixed flanges with simply supported stiffeners, and (iv) simply supported flanges with fixed stiffeners.

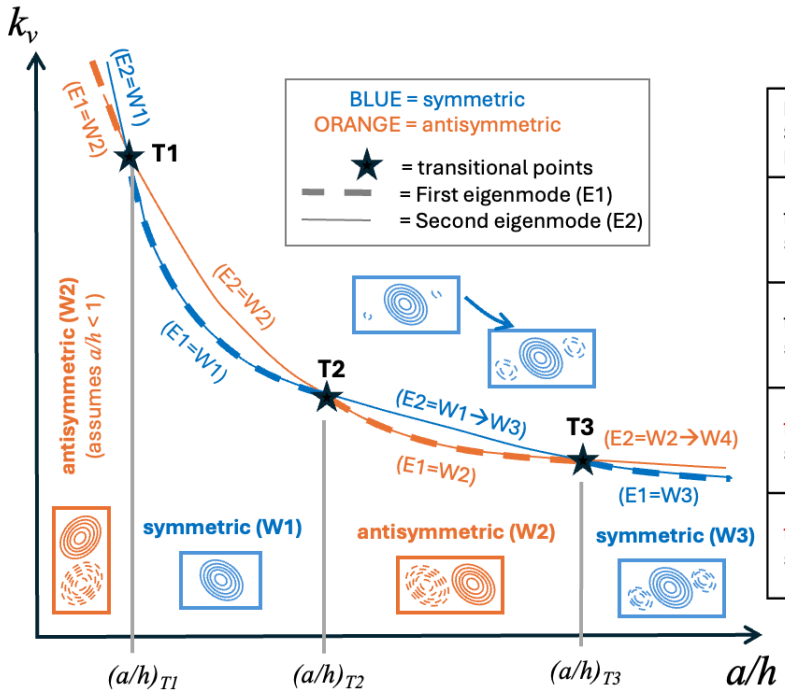

Boundary Condition S = simply supported F = fixed (clamped)		Transitional Values T1 (A→S)	T2 (S→A)	T3 (A→S)
flange = S stiffener = S	a/h	0.49	2.02	3.35
	$k_{v,SS}$	27.1	6.53	5.78
flange = F stiffener = F	a/h	0.61	1.63	2.51
	$k_{v,F}$	30.1	11.2	9.87
flange = F stiffener = S	a/h	0.42	1.33	2.22
	$k_{v,Ffl}$	36.7	11.5	9.92
flange = S stiffener = F	a/h	0.75	2.39	3.74
	$k_{v,Sfl}$	20.4	6.44	5.76

Figure 2: Conceptual relationship between k_v and a/h showing transitional values of a/h where the first eigenmode (the lower bound) shifts from antisymmetric to symmetric (or vice versa).

2.2. Nonlinear Shear Response

The nonlinear shear mechanics of stiffened webs in steel plate girders have been the subject of extensive experimental and numerical research (Masungi et al. 2025; Scandella et al. 2020, Masungi et al. 2024a; Ahdab 2024; Augustyn et al. 2022; Hingnekar and Vyavahare 2020). Accordingly, only a concise summary is provided herein, and readers are referred to the cited studies for more detail. The shear response of a stiffened web panel can be described by three sequential stages, which collectively define three possible response mechanisms, as illustrated schematically in Fig. 3. These stages capture the transition from elastic behavior to inelastic web action and then, ultimately, to frame-dominated response. In Stage 1, the elastic response stage, the web panel deforms out of plane due to the presence of initial geometric imperfections. Stage 1 concludes at the elastic limit milestone, shear load V_{el}, which corresponds to the end of a linear response (i.e., when a noticeable change in stiffness is observed) due to the *surface* of the web yielding along the tension diagonal. This yielding is a combination of tensile membrane stresses along the diagonal and compression-induced second-order bending stresses. Note that depending on the girder geometry, V_{cr} based on Eq. 1 may be either lower or higher than V_{el}, as illustrated in

Fig. 3.

Stage 2 is the web yielding stage and begins after V_{el}. In this nonlinear stage, yielding progressively saturates through the web plate thickness along the tension diagonal, while out-of-plane deformations continue to increase due to compression-induced second-order bending. Stage 2 terminates at the milestone load V_w, which is defined herein as the "*shear capacity*" of the plate girder web. The value V_w corresponds to the first peak in the shear load–displacement response, when the global shear stiffness reduces to zero (Masungi et al. 2025, Numanović and Knobloch 2025b, Augustyn et al. 2022). This milestone occurs when the web has yielded through its *full thickness* along the length of the tension diagonal. Defining V_w as the shear capacity is physically meaningful since the web typically resists most of the applied shear up to this point. Certain geometric configurations, particularly those with relatively stiff flanges and transverse stiffeners, may sustain additional shear beyond V_w; however, the associated strength gain is generally modest and occurs at substantially larger displacements (Masungi et al. 2025). Thus, in those cases, defining V_w as the shear capacity is only slightly conservative.

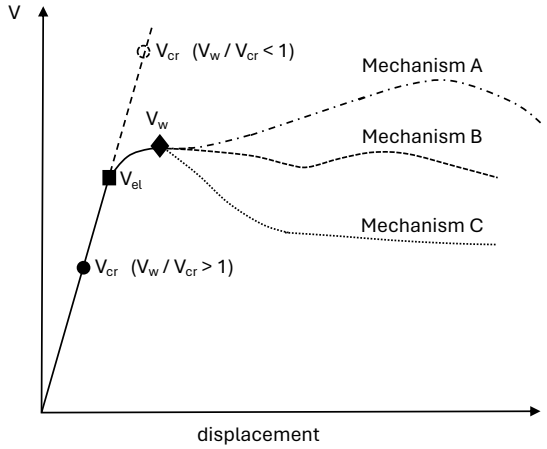

Figure 3: Genetic schematic of the global shear response of plate girders.

Finally, the response beyond V_w enters Stage 3, during which the panel's boundary framing becomes increasing engaged. In this stage, the web is no longer capable of carrying additional shear, and the load path progressively shifts to the surrounding frame elements (i.e., the flanges and transverse stiffeners). The post V_w response heavily depends on the stiffness and strength of these frame elements and typically follows one of three mechanisms shapes (see Fig. 3).

2.3. Influence of Initial Imperfection Eigenmode Shape

The appropriate shape and magnitude of initial imperfections have been the focus of numerous numerical investigations (Masungi et al. 2024a; Ahdab; Augustyn et al. 2022; Lee and Yoo 1998; Ghadami and Broujerdian 2019; Bergfelt 1979). In most of those studies, initial out-of-flatness web imperfections are represented by scaling an elastic buckling eigenmode shape to a prescribed maximum amplitude. It is commonly assumed that E1, which defines the lower-bound elastic shear buckling load V_{cr}, will also lead to the lower-bound inelastic shear capacity V_w.

However, this assumption has been disproved in recent studies (Masungi et al. 2025; Ahdab et al. 2025). Masungi et al. (2024b) conducted field measurements of initial out-of-flatness

imperfections on 12 fabricated steel plate girders with web depths ranging from 0.91 to 2.08 m. The measured imperfections exhibited substantial variability and were typically highly localized and dimple-like rather than globally smooth. When only the maximum imperfection *per panel* was considered, the average magnitude was approximately $d/170$, where $d = \min(a, h)$. However, a statistical evaluation of the full dataset of many panels yielded a much smaller mean imperfection magnitude of approximately $d/835$, highlighting the localized nature of fabrication-induced imperfections.

Building on these measurements, Masungi et al. (2024a) evaluated the influence of imperfection magnitude and shape on the shear capacity of steel plate girders using finite element models. Two categories of imperfections were considered: (i) directly measured field geometries and (ii) idealized eigenmode shapes (E1 and E2) that were scaled to the maximum permitted out-of-flatness per the AASHTO/AWS D1.5 Bridge Welding Code (AASHTO 2020). The results of those analyses indicated that eigenmode-based imperfections with maximum magnitudes between $d/300$ and $d/600$ were generally suitable for nonlinear FE analyses, by producing shear capacities consistent with models that incorporated field-measured imperfections. However, no definitive recommendation was made regarding whether E1 or E2 should be used as the imperfection shape, since either mode could govern the inelastic response depending on the girder geometry.

This observation was further explored by Masungi et al. (2025) via numerical modeling of 28 large-scale shear tests. For each test, two finite element analyses were performed: one using E1 and one using E2 as the initial imperfection shape, both scaled to a maximum amplitude of $d/300$. Overall, the finite element predictions using either eigenmode exhibited good agreement with the experimental data, with most results falling within 0.8 to 1.1 of the measured shear capacities. Importantly, however, the study demonstrated that the eigenmode producing the controlling (lowest) shear capacity was not consistent – in some cases, E1 controlled, while in others E2 controlled.

More recently, Ahdab et al. (2025) extended this work using a dataset of 929 unique panel geometries derived from a database of commercially fabricated steel plate girders over the period of 2013-2023. These results demonstrated that the shape of the initial imperfection (that is, the number of half-waves) is more influential than the eigenmode (E1 or E2) in determining the *controlling* shear capacity, $V_{w,C}$. While the first eigenmode represents the minimum-energy (i.e. lower bound) configuration in the elastic regime, it does not necessarily represent the minimum energy in the nonlinear regime. For example, in the eigensystem study, the first eigenmode may exhibit two half-waves, whereas the inelastic shear capacity may be controlled by a one half-wave deformation pattern, or vice vera.

Accordingly, Ahdab et al. (2025) found that the initial imperfection selected for these numerical simulations should correspond to the eigenmode (E1 or E2) that best represents the controlling deformation shape, symmetric or antisymmetric, associated with the governing inelastic shear capacity $V_{w,C}$, rather than simply defaulting to E1. This controlling shape can be identified as a function of a/h and h/t_w (Ahdab et al. 2025) – for instance, when $h/t_w < 100$, the choice of eigenmode shape has a negligible influence on the shear response. However, for slender webs with $h/t_w > 100$ and approximately $1.6 \leq a/h \leq 2.5$, the final deformed configuration at shear

capacity more closely resembles that of E2.

Although these studies have significantly advanced our understanding of imperfection sensitivity in stiffened plate girder webs, a comprehensive investigation is still needed to simultaneously consider theoretical elastic buckling characteristics (including eigenvalues and eigenmode shapes) and realistic, field-measured imperfections, and their combined influence on both the elastic shear buckling load V_{cr} and the inelastic shear capacity V_w. The primary objective of this study is therefore to clarify the role of the elastic eigensystem and field-measured imperfections in the inelastic shear response of steel plate girder web panels.

3. Finite Element Modeling and Prototypes

Finite element (FE) modeling has played a central role in advancing the understanding of these mechanics. While full-span girder models can accurately capture shear behavior, their computational cost limits their use in large parametric studies. Consequently, many researchers have adopted isolated web panel models subjected to pure shear, with boundary conditions either explicitly modeled or idealized (Ahdab et al. 2025; Kim 2014; Masungi et al. 2024a; Garlock et al. 2019; Wang et al. 2021; Yoo and Lee 2006; Augustyn et al. 2023; Xiao et al. 2018; Ahdab 2024; Glassman et al. 2016b; Pedro et al. 2025; Numanović and Knobloch 2025b; Nayak and Subramanian 2025; Nayak and Subramanian 2024; Augustyn et al. 2022; Lee and Yoo 1998; Ghadami and Broujerdian 2019; Gomez 2020; Lee et al. 1996; Marsh et al. 1988). Among these approaches, the extended panel model (EPM), described next, has proven to be both efficient and reliable (Wang et al. 2021).

3.1. Extended Panel Model Approach

The FE modeling approach for this study utilizes the Extended Panel Model (EPM) (Fig. 4), which is commonly used to investigate both the theoretical elastic shear buckling and realistic inelastic shear behavior of stiffened steel plate girder webs. Each model represents an interior web panel and extends a longitudinal distance of $d/2$ beyond each transverse stiffener to allow realistic stress continuity and boundary restraint, consistent with the recommendations of Wang et al. (2021). This modeling approach has been previously validated by Masungi et al. (2025) against 28 experimental tests and has been shown to accurately capture both elastic buckling behavior and nonlinear shear response.

Boundary conditions are applied exclusively to the stiffened web panel. To simulate a state of pure shear, a uniform shear force per unit length is applied along all four edges of the web panel (Wang et al. 2019). Welded connections between the web, flanges, and transverse stiffeners are modeled using node-based surface tie constraints in ABAQUS (Dassault Systemes Simulia Corp 2025). These constraints are applied along the web-to-flange, web-to-stiffener, and flange-to-stiffener interfaces and enforce full translational and rotational compatibility at coincident nodes. This connection modeling strategy has been successfully adopted in several prior numerical studies of plate girders (Ahdab et al. 2025; Masungi et al. 2025; Augustyn et al. 2023; Augustyn et al. 2022).

Initial imperfections are introduced directly into the nodal geometry of the FE models prior to nonlinear analysis, avoiding the need for artificial local forces or imposed displacements and ensuring a stress-free initial configuration. Consistent with previous research by the authors and others (Ahdab et al. 2025, Masungi et al. 2025, Masungi et al. 2024a, Wang et al. 2021, Augustyn

et al. 2023, Ahdab 2024, Augustyn et al. 2022), residual stresses are neglected, as their influence on the shear response of plate girder webs has been shown to be minimal. In contrast, inclusion of initial out-of-flatness imperfections is essential for accurately reproducing experimentally observed shear behavior. Accordingly, each imperfection is defined by both its shape and magnitude. This study primarily considers the E1 and E2 positive eigenmode shapes obtained from linear buckling analysis, as well as field-measured imperfection geometries reported by Masungi et al. (2024a). For eigenmode-based imperfections, a conservative maximum imperfection magnitude of $d/300$ is applied per the recommendations of Masungi et al. (2024a). For field-measured imperfection shapes, the maximum measured out-of-flatness is directly applied.

Linear elastic eigenvalue buckling analyses produce the elastic shear buckling eigenvalues and corresponding eigenmode shapes. These results are used to compute the elastic critical shear buckling load V_{cr}. The nonlinear simulations include geometric and material nonlinearity, and use the Modified Riks (arc-length) method in ABAQUS (Dassault Systemes Simulia Corp 2025). This approach enables tracing of the equilibrium response beyond initial buckling and into the nonlinear regime, allowing the determination of the shear capacity V_w.

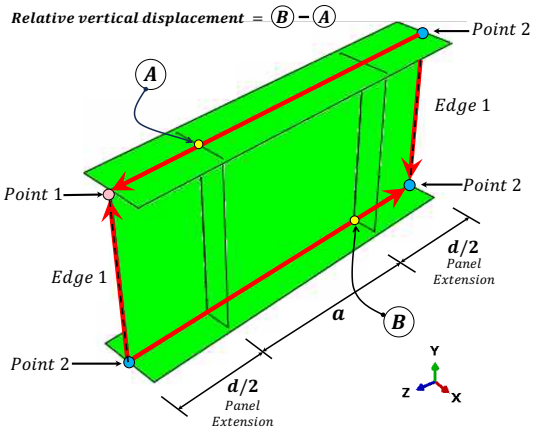

	U_x	U_y	U_z	UR_x	UR_y	UR_z
Point 1 ○	X	X	X	X	X	X
Point 2 ●	X			X	X	X
Edge 1 ---	X			X		X

Figure 4: FE representation of an extended panel model (EPM). Panel extensions equal $d/2$, where d = minimum of h and a.

All plates are modeled using four-node quadrilateral S4 shell elements, which capture both membrane and bending actions and are formulated for finite-strain applications. Five integration points are specified through the thickness to adequately capture nonlinear stress distributions, (Garlock et al. 2019). A uniform mesh with a target edge dimension of $h/50$ is used for all models, based on prior convergence studies for both elastic and inelastic shear response (Garlock et al. 2019, Wang et al. 2019). All steel components are modeled using an elastoplastic, strain-hardening material model with isotropic hardening and a multi-linear stress–strain relationship capturing elastic behavior, yielding, and post-yield ductile deformation (see Masungi et al. (2024a) for more information). The material properties used throughout the study are nominal values: modulus of elasticity E = 200 GPa, yield strength F_y = 345 MPa, and Poisson's ratio μ=0.3.

3.2. Prototypes

The study considers three plate girders shown in Table 1: two from a commercial fabrication shop, designated G3W and G4W (whose web panels were measured and documented by Masungi et al. (2024a, 2024b)); and one experimental specimen documented by Masungi et al. (2025). The G3W and G4W girders each consider two interior web *panels* with distinct measured imperfection geometries, while the experimental specimen girder considers only one panel; thus, 5 web panels are examined, each with unique measured imperfections. The geometric properties and measured web imperfections are summarized in Table 1, which shows that these girders have a large range of field-measured imperfection shapes and magnitudes. The h/t_w ranges from 118 to 138, and a/h is relatively consistent, ranging from only 2.00 to 2.29.

Table 1: Geometric properties of prototypes and their field-measured imperfections.

Plate Girder	h/t_w	a/h	h (mm)	t_w (mm)	a (mm)	**Panel**	**Measured Imperfection**		
							Name	**Shape**	**Max. Magnitude**
G3W	118	2.02	1,880	15.9	3,800	Panel 1	P1-I	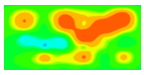	$d/198$
						Panel 2	P2-I	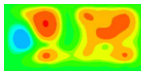	$d/188$
G4W	109	2.29	2,080	19.1	4,777	Panel 1	P1-I	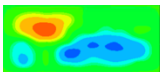	$d/241$
						Panel 2	P2-I	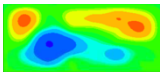	$d/190$
Masungi et al. 2025	138	2.00	1,753	12.7	3,505	Panel 1	P1-I	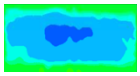	$d/88$
							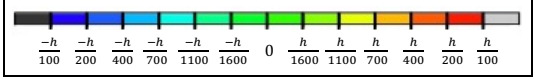		

4. Elastic Response (Analyses of V_{cr} and Shapes)

This section examines the elastic shear buckling response of the web panels in Table 1 via linear eigenvalue buckling analyses with two initial conditions on the web plate: (i) perfectly flat and (ii) field-measured initial imperfections. Table 2 summarizes the results. As expected, the linear buckling analyses for the flat web initial condition reproduced the classical symmetric and antisymmetric half-wave buckling patterns that have been widely reported in the literature (Timoshenko and Gere 2009; Stein and Neff 1947; Chilver 1967; Budiansky 1948; Gerard and Becker 1957; Cook and Rockey 1962a, 1962b; Budiansky et al. 1948; Ahdab et al. 2025). Since the panel aspect ratios are all similar (see Table 1), the eigenmode shapes are all the same (see Fig. 2): an antisymmetric E1, corresponding to a W2 shape; and a symmetric E2, transitioning from W1 to W3. In contrast, the initial condition with field-measured imperfection geometries produced markedly different eigenmode shapes. Rather than forming symmetric or antisymmetric half-wave patterns, the resulting eigenmodes were characterized by multiple localized, dimple-like out-of-flatness deformations distributed across the panel.

The V_{cr} values for webs with field-measured initial conditions were five to seven times larger than

those for perfectly flat web plates. An elastic shear buckling bifurcation is thus unlikely to occur in plate girder webs, since inelastic (yield) failure is likely to be reached well before elastic buckling given realistic initial conditions (imperfections). Further, Table 2 shows that using measured initial conditions (P1-I and P2-I) for girders G3W and G4W resulted in similar eigenmode characteristics and elastic shear buckling loads, with differences in V_{cr} of less than 1%, despite differing initial condition patterns. This observation suggests that geometric parameters, such as h, a, and t_w, may play a more dominant role than the precise spatial distribution of field imperfections in governing the elastic buckling response when realistic imperfection shapes are considered.

Table 2: Linear buckling analysis results for prototype web panels with two initial conditions: flat and imperfections.

Plate Girder	**Initial Condition (Scale #1)**	**Linear buckling analysis results**		**Initial Imperfection for nonlinear**
		Eigenmode (Scale #2)	V_{cr} (KN)	
G3W	Flat Web	**(E1)** 1st Eigenmode 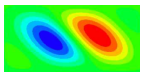	3,796	E1
		(E2) 2nd Eigenmode 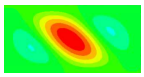	3,914	E2
	Measured Imperfections **(P1-I)** Panel 1 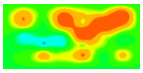	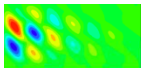	25,402	P1-I
	(P2-I) Panel 2 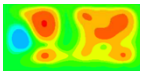	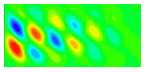	25,626	P2-I
G4W	Flat Web	**(E1)** 1st Eigenmode 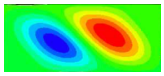	5,325	E1
		(E2) 2nd Eigenmode 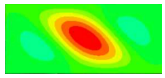	5,451	E2
	Measured Imperfections **(P1-I)** Panel 1 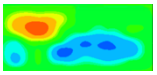	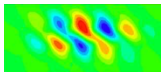	28,179	P1-I
	(P2-I) Panel 2 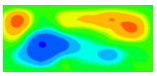	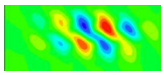	28,385	P2-I
Masungi et al. 2025	Flat Web	**(E1)** 1st Eigenmode 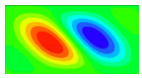	2,162	E1
		(E2) 2nd Eigenmode 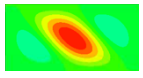	2,224	E2
	Measured Imperfections **(P1-I)** Panel 1 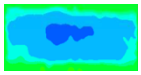	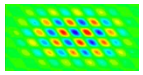	15,495	P1-I

Scale #1: Field-Measured Imperfection Shape

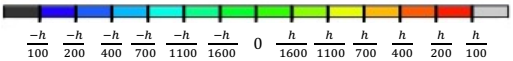

Scale #2: Eigenmode Shape

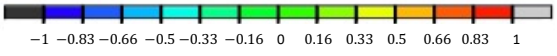

5. Nonlinear Response (Analyses of V_w and Shapes)

The nonlinear shear response of the prototype web panels was evaluated using initial imperfections noted in the last column of Table 2: (i) the E1 and E2 shapes obtained from linear buckling analyses of perfectly flat web plates, each applied with a conservative maximum imperfection magnitude of $d/300$ (as described in Section 3.1); and (ii) field-measured imperfection geometries, applied using their recorded out-of-flatness magnitudes. The first approach is often used when the true imperfections are unknown, whereas the second is representative of true field conditions.

Table 3: Shear capacity,V_w, results using various initial imperfections.

	Initial Imperfection			**Shear Capacity Results**			
Model Name	**Basis**	**Max. Magnitude**	**Initial Shape (Scale #1)**	**Shape at V_w (Scale #2)**	**V_w (kN)**	**$\frac{V_w}{V_{w,E1}}$**	**$\frac{V_w}{V_{w,E2}}$**
G3W (E1)	Eigen-mode	$d/300$	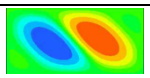	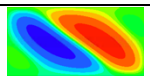	**4,307**	1.00	1.00
G3W (E2)		$d/300$	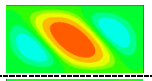	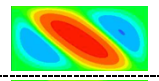	4,316	1.00	1.00
G3W (P1-I)	Field Meas.	$d/198$	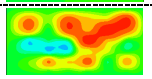	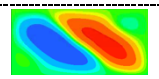	4,384	1.02	1.02
G3W (P2-I)		$d/188$	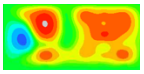	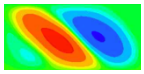	4,402	1.02	1.02
G4W (E1)	Eigen-mode	$d/300$	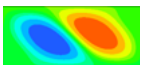	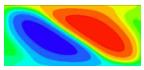	**5,694**	1.00	0.98
G4W (E2)		$d/300$	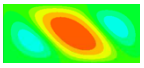	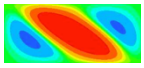	5,807	1.02	1.00
G4W (P1-I)	Field Meas.	$d/241$	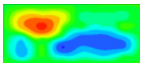	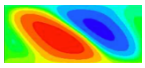	5,840	1.03	1.01
G4W (P2-I)		$d/190$	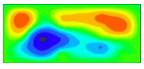	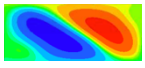	5,935	1.04	1.02
Masungi (E1)	Eigen-mode	$d/300$	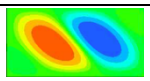	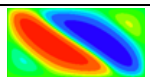	3,520	1.00	1.02
Masungi (E2)		$d/300$	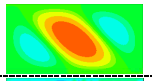	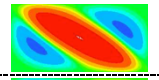	**3,438**	0.98	1.00
Masungi (P2-I)	Field Meas.	$d/88$	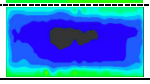	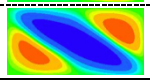	3,438	0.98	1.00
	Scale #1: Initial Imperfection Shape		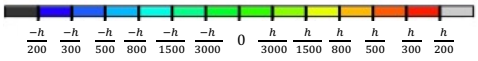	**Scale #2: Shape at V_w**	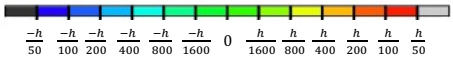		

Results are shown in Table 3, where the following is observed:

- When eigenmode-based imperfections (E1 and E2) are used, the final deformed shape at V_w closely matches the eigenmode-based imperfection shape for all three cross-sections.
- When field-measured imperfection shapes are used in cross-sections G3 and G4, Panels 1 and 2 exhibit final deformed shapes at V_w that are similar to one another.
- In all three cross-sections, when measured imperfections are used, the final deformed shape at V_w is similar to the controlling eigenmode initial imperfection shape (i.e., the eigenmode that produces the smaller of $V_{w,E1}$ and $V_{w,E2}$). For example, the E1 imperfection controls G3W and

G4W since it produces the smallest V_w, whereas E2 controls the Masungi et al. cross-section.
- Using measured initial imperfections leads to V_w that ranges from 1.00 to 1.04 times the V_w based on the controlling eigenmode imperfection scaled to $d/300$.
- Employing an eigenmode-based imperfection shape (either E1 or E2) with a maximum imperfection magnitude of $d/300$ can accurately predict both the inelastic shear capacity V_w magnitude and shape of panels that incorporate realistic, field-measured imperfections.

6. Effect of Slenderness Ratio on Elastic and Nonlinear Response

The influence of web slenderness ratio h/t_w on both the linear elastic buckling response and the nonlinear inelastic shear response is investigated systematically by varying the web thickness t_w on girder G3W while maintaining the web height at a constant value of 1,880 mm. Specifically, the original G3W model had $h/t_w = 118$ with $t_w = 15.9$ mm and was modified by reducing the web thickness to $t_w = 12.7, 9.4,$ and 7.5, resulting in $h/t_w = 148, 200,$ and 250, respectively. In addition, the same field-measured imperfection geometry is applied in all cases to isolate the effect of web slenderness.

6.1. Elastic Response

Replicating the approach presented previously in Section 4, linear eigenvalue buckling analyses are again performed using two initial conditions: (i) perfectly flat web plates and (ii) web plates incorporating field-measured initial imperfection geometries. Table 4 summarizes the elastic buckling results for G3W over the range of h/t_w values considered. When the initial condition is a perfectly flat web plate, as expected, the linear buckling analyses result in classical symmetric and antisymmetric half-wave buckling patterns, and these eigenmode shapes remain unchanged as h/t_w increases. In contrast, when the initial condition includes imperfections in the web, the eigenmode shapes are significantly different. As discussed in Section 4, these resulting eigenmodes are again characterized by multiple dimple-like deformations distributed across the web panel. This response is similar for all values of h/t_w.

When comparing the V_{cr} values for the E1 and E2 models, the value for E2 is about 3% larger than for E1, which is consistent with the results of Ahdab et al. (2025) for $a/h \approx 2$. For Panels 1 and 2, which have different field-measured imperfections as initial conditions, the difference in V_{cr} is less than 1%. As expected, increasing h/t_w (by decreasing t_w) results in a reduction in V_{cr}. Across all h/t_w values, the elastic shear buckling loads V_{cr} for the field-measured imperfection initial condition are 6.7 times larger on average than those for the flat plate initial condition. This result supports the conclusions of Section 4, which indicates that for the geometries studied, an elastic shear buckling bifurcation is unlikely to occur in plate girder webs, since inelastic (yield) failure is likely to be reached well before elastic buckling given realistic initial conditions (imperfections).

The results of this elastic eigensystem study indicate that, while increasing web slenderness significantly affects the magnitude of V_{cr}, it does not substantially alter the elastic buckling deformation patterns, regardless of whether the response is characterized using eigenmodes of perfectly flat plates or using eigenmodes arising from field-measured imperfections. Furthermore, V_{cr} increases nearly seven-fold when field-measured initial imperfections are included; thus, the relevance of V_{cr} as a limit state affecting the behavior of plate girders should be reexamined. For this reason, V_{cr} is assumed herein to represent only a theoretical or mathematical construct and not a physical one.

Table 4: Varying h/t_w on Plate Girder G3W: linear buckling analysis results.

	Linear Buckling Analysis Results (Scale #2)			
Initial Condition (Scale #1)	$h/t_w = 118$[(1)]	$h/t_w = 148$	$h/t_w = 200$	$h/t_w = 250$
Flat Web — (E1) 1st Eigenmode	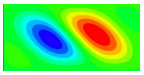 $V_{cr} =$ 3,796 kN	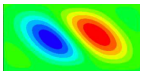 $V_{cr} =$ 1,977 kN	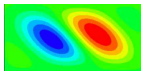 $V_{cr} =$ 812 kN	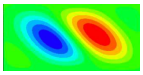 $V_{cr} =$ 414 kN
Flat Web — (E2) 2nd Eigenmode	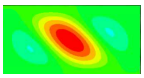 $V_{cr} =$ 3,914 kN	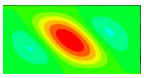 $V_{cr} =$ 2,035 kN	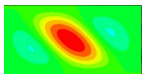 $V_{cr} =$ 835 kN	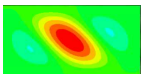 $V_{cr} =$ 427 kN
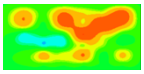 P1-I	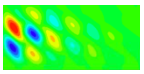 $V_{cr} =$ 25,402 kN	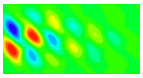 $V_{cr} =$ 13,268 kN	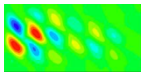 $V_{cr} =$ 5,508 kN	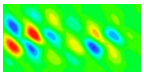 $V_{cr} =$ 2,837 kN
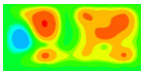 P2-I	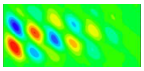 $V_{cr} =$ 25,626 kN	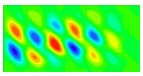 $V_{cr} =$ 13,339 kN	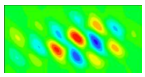 $V_{cr} =$ 5,518 kN	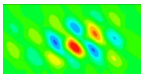 $V_{cr} =$ 2,833 kN
Scale #1: Field-Measured Imperfection Shape 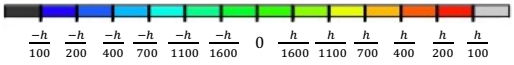 $\frac{-h}{100}$ $\frac{-h}{200}$ $\frac{-h}{400}$ $\frac{-h}{700}$ $\frac{-h}{1100}$ $\frac{-h}{1600}$ 0 $\frac{h}{1600}$ $\frac{h}{1100}$ $\frac{h}{700}$ $\frac{h}{400}$ $\frac{h}{200}$ $\frac{h}{100}$		**Scale #2: Eigenmode Shape** 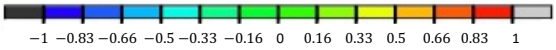 −1 −0.83 −0.66 −0.5 −0.33 −0.16 0 0.16 0.33 0.5 0.66 0.83 1		

Note (1): Original G3W model, same as in Table 2

6.2. Nonlinear Response

Replicating the approach presented previously in Section 5, the nonlinear shear response of the G3W web panels with varying slenderness ratios was evaluated by examining the shear capacity V_w. Two categories of initial imperfection shapes were again considered: (i) the first and second eigenmode shapes (E1 and E2) obtained from linear buckling analyses of perfectly flat web plates (see Table 4), each applied with a conservative maximum imperfection magnitude of $d/300$, as described in Section 3.1; and (ii) field-measured imperfection geometries, applied using their recorded out-of-flatness magnitudes. The results are summarized in Table 5. Note that for $h/t_w = 250$, only Panel 1 is included since the analysis using the field-measured imperfection corresponding to Panel 2 exhibited numerical convergence difficulties, likely due to the high slenderness.

For analyses with eigenmode-based initial imperfections (E1 and E2), the final deformed shape at the inelastic shear capacity V_w is similar to that for the imposed initial imperfection shape across all slenderness models. As h/t_w increases, the eigenmode that governs V_w transitions from E1 (at $h/t_w = 118$) to E2 at larger values of h/t_w. This transition is consistent with the trends reported by Ahdab et al. (2025).

For analyses with field-measured initial imperfections (P1-I and P2-I), those with lower slenderness ratios ($h/t_w = 118$ and 148) exhibit nearly identical deformation patterns at V_w, despite having different spatial distributions of imperfections. These results are consistent with observations discussed in Section 5. However, at $h/t_w = 200$, the P1-I imperfection develops an

antisymmetric deformation pattern (i.e., two major bulges) at V_w, whereas P2-I exhibits a symmetric deformation pattern (i.e., one major bulge and two minor ones). These results suggest that, at higher web slenderness ratios, the final deformation shape at V_w is governed not only by global panel geometry but also by the characteristics of the initial imperfection distribution. Across all cases considered, the shear capacities V_w obtained using eigenmode-based imperfections and those obtained using field-measured imperfection geometries differ by less than 5%.

Table 5: G3W EPM V_w results for varying h/t_w using E1 and E2 eigenmode imperfections compared with those for Panel 1 and Panel 2 field-measured imperfection shapes.

		Shear Capacity Results (Scale #2)			
Model Name	**Initial Imperfection (Scale #1)**	$h/t_w = 118$[(1)]	$h/t_w = 148$	$h/t_w = 200$	$h/t_w = 250$
G3W (E1)	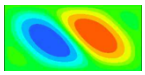 E1 (max $d/300$)	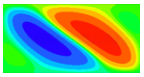 **V_w = 4,307 kN** $V_w/V_{w,E1}$ = 1.00 $V_w/V_{w,E2}$ = 1.00	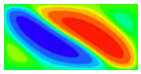 V_w = 3,005 kN $V_w/V_{w,E1}$ = 1.00 $V_w/V_{w,E2}$ = 1.01	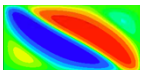 V_w = 1,869 kN $V_w/V_{w,E1}$ = 1.00 $V_w/V_{w,E2}$ = 1.05	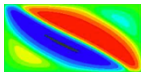 V_w = 1,345 kN $V_w/V_{w,E1}$ = 1.00 $V_w/V_{w,E2}$ = 1.02
G3W (E2)	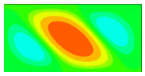 E2 (max $d/300$)	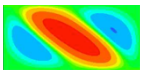 V_w = 4,316 kN $V_w/V_{w,E1}$ = 1.00 $V_w/V_{w,E2}$ = 1.00	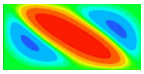 **V_w = 2,964 kN** $V_w/V_{w,E1}$ = 0.99 $V_w/V_{w,E2}$ = 1.00	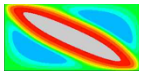 **V_w = 1,778 kN** $V_w/V_{w,E1}$ = 0.95 $V_w/V_{w,E2}$ = 1.00	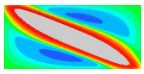 **V_w = 1,316 kN** $V_w/V_{w,E1}$ = 0.98 $V_w/V_{w,E2}$ = 1.00
G3W (P1-I)	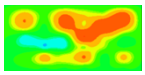 Field-measured (max $d/198$)	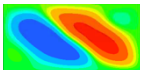 V_w = 4,384 kN $V_w/V_{w,E1}$ = 1.02 $V_w/V_{w,E2}$ = 1.02	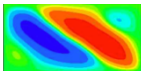 V_w = 3,005 kN $V_w/V_{w,E1}$ = 1.00 $V_w/V_{w,E2}$ = 1.01	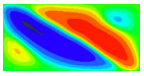 V_w = 1,838 kN $V_w/V_{w,E1}$ = 0.98 $V_w/V_{w,E2}$ = 1.03	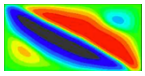 V_w = 1,330 kN $V_w/V_{w,E1}$ = 0.99 $V_w/V_{w,E2}$ = 1.01
G3W (P2-I)	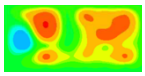 Field-measured (max $d/188$)	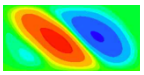 V_w = 4,402 kN $V_w/V_{w,E1}$ = 1.02 $V_w/V_{w,E2}$ = 1.02	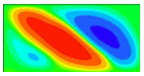 V_w = 2,995 kN $V_w/V_{w,E1}$ = 1.00 $V_w/V_{w,E2}$ = 1.01	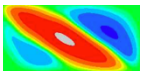 V_w = 1,782 kN $V_w/V_{w,E1}$ = 0.95 $V_w/V_{w,E2}$ = 1.00	NA
Scale #1: Initial Imperfection Shape 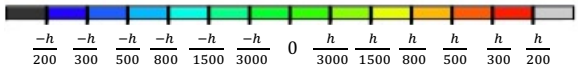 $\frac{-h}{200}$ $\frac{-h}{300}$ $\frac{-h}{500}$ $\frac{-h}{800}$ $\frac{-h}{1500}$ $\frac{-h}{3000}$ 0 $\frac{h}{3000}$ $\frac{h}{1500}$ $\frac{h}{800}$ $\frac{h}{500}$ $\frac{h}{300}$ $\frac{h}{200}$				**Scale #2: Shape at V_w** 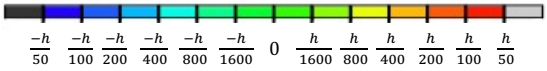 $\frac{-h}{50}$ $\frac{-h}{100}$ $\frac{-h}{200}$ $\frac{-h}{400}$ $\frac{-h}{800}$ $\frac{-h}{1600}$ 0 $\frac{h}{1600}$ $\frac{h}{800}$ $\frac{h}{400}$ $\frac{h}{200}$ $\frac{h}{100}$ $\frac{h}{50}$		

Note (1): Original G3W model, same as in Table 3

Collectively, the results for G3W demonstrate that employing conservative eigenmode-based imperfection shapes (E1 or E2) with a maximum imperfection magnitude of $d/300$ can accurately reproduce both the inelastic shear capacity V_w and the governing deformation patterns of models that incorporate field-measured imperfections over a wide range of h/t_w values. These findings confirm the robustness and effectiveness of eigenmode-based imperfections within a numerical framework for predicting actual inelastic web shear behavior.

7. Summary and Conclusions

This study examined the role of initial geometric imperfections and web slenderness in governing the elastic buckling and inelastic shear capacity of steel plate girder web panels. Experimentally validated finite element models representing interior web panels were developed based on a dataset of five web panels from three commercially fabricated plate girders with field-measured imperfections. These imperfections were used in elastic buckling analyses and compared to flat plates as the initial condition. They were also used in nonlinear analyses and compared to eigenmode-shaped imperfections. In addition, a parametric study was conducted in which the web slenderness of selected panels was increased while all other geometric parameters and imperfection shapes were held constant.

The main conclusions of this study are limited to the aforementioned geometries and can be summarized as follows:

- Across all slenderness ratios, the elastic shear buckling load, V_{cr}, obtained from linear buckling analyses of webs with realistic, field-measured imperfections is on the order of 5 to 7 times larger than that for perfectly flat webs. This result indicates that a distinct elastic shear buckling bifurcation is unlikely to occur in the shear response of real plate girder webs, since the web plate will contain some form of imperfection. The relevance of V_{cr} as a limit state affecting the behavior of plate girders should be reconsidered, as it may represent only a theoretical or mathematical construct.
- Using different measured initial conditions on the same plate girder resulted in similar eigenmode characteristics and differences in V_{cr} of less than 1%. This observation suggests that the precise spatial distribution of field imperfections does not significantly influence the elastic buckling response.
- In nonlinear analyses, when eigenmode-based initial imperfections are employed, the deformed shape at the shear capacity, V_w, is similar to the initial imperfection shape. However, when measured imperfections are used, the final deformed shape at V_w for webs with lower slenderness is similar to the governing eigenmode shape (i.e., the eigenmode (E1 or E2) that produces the smaller of $V_{w,E1}$ and $V_{w,E2}$).
- As web slenderness increases, the controlling deformation pattern at V_w may transition between antisymmetric and symmetric shapes, and the influence of imperfection shape becomes more pronounced. Even in these slender cases, eigenmode-based imperfections with a conservative maximum imperfection magnitude of $d/300$ enable accurate estimates of V_w versus those made using measured imperfections.

The results of this study highlight the need for future work that broadens the range of geometries and imperfections from those examined here. Such an extended study can then provide insights for developing design recommendations that more accurately account for the role of imperfections in the shear response of stiffened steel plate girders.

Acknowledgments

The authors would like to acknowledge former doctoral student Parfait Masungi for collecting the field measurements of steel plate girder webs used in this study.

References

AASHTO. (2020). "AASHTO/AWS D1.5M/D1.5:2020 Bridge Welding Code", *8th Edition. Washington, D.C.: American Association of State Highway and Transportation Officials*.

Ahdab M.D. "REDEFINING THE SHEAR CAPACITY OF STEEL PLATE GIRDERS BASED ON RECENT SHEAR MECHANICS AND AN EXTENSIVE NUMERICAL INVESTIGATION" (2024). *Master's Thesis. Princeton University*.

Ahdab M.D., Garlock M.E.M., Quiel S.E. (2025). "Shear Resistance of Stiffened Steel Plate Girders: Influence of Eigensystems on Inelastic Response." *Thin-Walled Structures*.

Augustyn K.E., Quiel S.E., Garlock M.E.M. (2022). "Post-buckling shear resistance of slender girder webs: Stiffener participation and flange contributions." *Journal of Constructional Steel Research*; 190:107117. https://doi.org/10.1016/j.jcsr.2021.107117.

Augustyn K.E., Quiel S.E., Garlock M.E.M. (2023). "Formation of post-buckling shear mechanisms in stiffened web panels of slender steel plate girders." *Thin-Walled Structures*; 184:110481. https://doi.org/10.1016/j.tws.2022.110481.

Basler K. (1961). "Shear Plate Girder." *Bethlehem, PA: Lehigh University*.

Bergfelt A., Hovik J. (1968). "Thin-walled deep plate girders under static loads." *IABSE*.

Bergfelt A. (1979). "Patch loading on a slender web-influence of horizontal and vertical stiffeners on the load carrying capacity". *Sweden: Chalmers University of Technology.*

Budiansky B. (1948). "BUCKLING STRESSES OF CLAMPED RECTANGULAR FLAT PLATES IN SHEAR."

Budiansky B., Hu P.C., Connor R.W. (1948). "Notes on the Lagrangian multiplier method in elastic-stability analysis."

Chilver A.H. (1967). "A Collection of Papers on the Stability and Strength of Thin-Walled Structural Members and Frames" *Thin-Walled Structures*, London: Chatto & Windus Ltd.

Cook I.T., Rockey K.C. (1962). "Shear Buckling of Clamped and Simply–Supported Infinitely Long Plates Reinforced by Transverse Stiffeners." *Aeronaut Q*; 13:41–70. https://doi.org/10.1017/S0001925900002249.

Cook I.T., Rockey K.C. (1963). "Shear Buckling of Rectangular Plates with Mixed Boundary Conditions." *Aeronaut Q*; 14:349–56. https://doi.org/10.1017/S0001925900002900.

Dassault Systemes Simulia Corp. "Abaqus/Standard" (2025).

Evans H.R., Porter D.M., Rockey K.C. (1978). "The collapse behaviour of plate girders subjected to shear and bending" https://doi.org/10.5169/SEALS-33222.

Freitas P., Nascimento S., Pedro J.J.O. (2024). "Shear buckling resistance and intermediate transverse stiffeners internal forces of full-scale steel plate girders – Experimental tests and numerical investigation." Eng*ineering Structures*; 314:118303. https://doi.org/10.1016/j.engstruct.2024.118303.

Garlock M.E.M, Quiel S.E., Wang P.Y., Alós-Moya J., Glassman J.D. (2019). "Post-Buckling Mechanics of a Square Slender Steel Plate in Pure Shear." *Eng J-Am Inst Steel Constr*; 56:27–46.

Gerard G., Becker H. (1957). "Handbook of Structural Stability Part I: Buckling of Flat Plates."

Ghadami A., Broujerdian V. (2019). "Shear behavior of steel plate girders considering variations in geometrical properties." *Journal Constructional Steel Research*; 153:567–77. https://doi.org/10.1016/j.jcsr.2018.11.009.

Glassman J.D., Garlock M.E.M., Aziz E.M., Kodur V.K. (2016). "Modeling parameters for predicting the postbuckling shear strength of steel plate girders." *Journal of Constructional Steel Research*; 121:136–43. https://doi.org/10.1016/j.jcsr.2016.01.004.

Gomez A. (2020). "Web Out-of-Straightness in Plate Girders: Methodology for Measurements and Effects on Shear Capacity." *Master's Thesis. Princeton University*.

Hansen T. (2018). "Post-buckling strength of plate girders subjected to shear - experimental verification." *Steel Construction*; 11:65–72. https://doi.org/10.1002/stco.201710035.

Hingnekar D.R., Vyavahare A.Y. (2020). "Mechanics of Shear Resistance in Steel Plate Girder: Critical Review." *Journal of Structural Engineering*; 146:03120001. https://doi.org/10.1061/(ASCE)ST.1943-541X.0002484.

Kamtekar A.G. (1972). "Tests on Hybrid Girders (Report 2)"

Kim D-W. (2014). "Shear Resistance of End Panels in Steel and Steel-Concrete Composite Plate Girders." *Dissertation. University of California, San Diego.*

Lee S.C., Davidson J.S., Yoo C.H. (1996). "Shear buckling coefficients of plate girder web panels." *Computation Struct*; 59:789–95. https://doi.org/10.1016/0045-7949(95)00325-8.

Lee S.C., Yoo C.H. (1998). "Strength of Plate Girder Web Panels under Pure Shear." *Journal of Structural Engineering*; 124:184–94. https://doi.org/10.1061/(ASCE)0733-9445(1998)124:2(184).

Lee S.C, Yoo C.H. (1999). "Experimental Study on Ultimate Shear Strength of Web Panels." *Journal Structural Engineering*; 125:838–46. https://doi.org/10.1061/(ASCE)0733-9445) 125:8(838).

Marsh C., Ajam W., Ha H-K. (1988). "Finite Element Analysis of Postbuckled Shear Webs." *Journal of Structural Engineering*; 114:1571–87. https://doi.org/10.1061/(ASCE)0733-9445(1988)114:7(1571).

Masungi P.M., Garlock M.E.M., Augustyn K.E., Quiel S.E. (2024a). "Out-of-Flatness of Steel Plate Girders Webs, Part II: Shear Strength and Behavior." *Journal Constructional Steel Research*.

Masungi P.M., Garlock M.E.M., Quiel S.E (2024b). "Out-of-flatness of steel plate girder webs, part I: Tolerance review and measurements." *Journal of Constructional Steel Research*; 215:108543. https://doi.org/10.1016/j.jcsr.2024.108543.

Masungi P.M., Ahdab M.D., Garlock M.E.M., Quiel S.E. (2025). "Efficacy of numerical models for capturing the local and global response of steel plate girders in shear." *Engineering Structures*; 340:120723. https://doi.org/10.1016/j.engstruct.2025.120723.

Nascimento S., Pedro J.J.O., Kuhlmann U. (2025). "Axial forces in transverse web stiffeners of steel plate girders – a numerical investigation." *Thin-Walled Structures*; 217:113778. https://doi.org/10.1016/j.tws.2025.113778.

Nayak N., Subramanian L.P. (2025). "Coupled Instabilities of Lateral Torsional Buckling and Shear Buckling of Singly Symmetric Steel I-Girders: Experimental and Numerical Investigations." *Journal of Bridge Engineering*; 30:04025017. https://doi.org/10.1061/JBENF2.BEENG-7258.

Nayak N., Subramanian L.P. (2024). "Steel I-girder geometries for enhanced stability in shear loading." *Journal of Constructional Steel Research*; 221:108906. https://doi.org/10.1016/j.jcsr.2024.108906.

Timoshenko S., Gere J.M. (2009)."Theory of elastic stability." *2nd ed., Dover ed*. Mineola, N.Y: Dover Publications.

Numanović M., Knobloch M. (2025a). "Web Shear Buckling of Steel-Concrete Composite Girders: Large-Scale Experimental Study." *Journal of Structural Engineering*; 151:04024194. https://doi.org/10.1061/JSENDH.STENG-13998.

Narayanan R, Rockey K. (1981). "Ultimate load capacity of plate girders with webs containing

circular cut-outs." *Proc Inst Civ Eng*; 71:845–62. https://doi.org/10.1680/iicep.1981.1822.
Numanović M., Knobloch M. (2025b). "Web shear buckling of steel-concrete composite girders – advanced numerical analysis." *Thin-Walled Structures*; 206:112671. https://doi.org/10.1016/j.tws.2024.112671.
Pedro J.O., Nascimento S., Hendy C. (2025a). "Shear Buckling Resistance Models for Steel Plate Girders – Numerical Investigation." https://doi.org/10.2139/ssrn.5148360.
Rockey K.C., Skaloud M. (1968). "Influence of flange stiffness upon the load carrying capacity of webs in shear." I*ABSE 8th Congr. Final Rep.*, Zürich, Switzerland: International Association for Bridge and Structural Engineering.
Sakai F. (1966). "Failure tests of plate girders using large-sized models."
Scandella C., Neuenschwander M., Mosalam K.M., Knobloch M., Fontana M. (2020). "Structural Behavior of Steel-Plate Girders in Shear: Experimental Study and Review of Current Design Principles." *Journal Structural Engineering*; 146:04020243. https://doi.org/10.1061/(ASCE)ST.1943-541X.0002804.
Stein M., Neff J. (1947). "Buckling stresses of simply supported rectangular flat plates in shear."
Wang P., Augustyn K., Gomez A., Quiel S., Garlock MEM. (2019). "Influence of boundary conditions on the shear post-buckling behavior of thin web plates." *Structural Stability Research Council (SSRC)*; p. 503–21.
Wang P.Y., Masungi P.M., Garlock M.E.M, Quiel S.E. (2021). "Postbuckling mechanics in slender steel plates under pure shear: A focus on boundary conditions and load path." *Thin-Walled Structures*; 169:108448. https://doi.org/10.1016/j.tws.2021.108448.
Xiao Y., Xue X.Y., Sun F.F., Li G.Q. (2018) "Postbuckling shear capacity of high-strength steel plate girders." *Journal of Constructional Steel Research*; 150:475–90. https://doi.org/10.1016/j.jcsr.2018.08.032.
Yoo C.H., Lee S.C. (2006). "Mechanics of Web Panel Postbuckling Behavior in Shear." *Journal of Structural Engineering*; 132:1580–9.